Traffic & Transportation

A Study on Traffic Flow Distribution in Road Networks Considering the Impact of Construction Zones

Shanhua ZHANG[1], Hong Ki AN[2], Choon Wah YUEN[3]

Original Scientific Paper
Submitted: 29 Aug 2024
Accepted: 24 Jan 2025

1 201203@jsei.edu.cn, School of Traffic and Transportation, Shijiazhuang Tiedao University, Shijiazhuang, China
2 Corresponding author, hongkian@unimap.edu.my, Faculty of Civil Engineering & Technology, Universiti Malaysia Perlis (UniMAP), Arau, Malaysia
3 yuencw@um.edu.my, Centre for Transportation Research, Department of Civil Engineering, Faculty of Engineering, Universiti Malaya, Kuala Lumpur, Malaysia

Publisher:
Faculty of Transport and Traffic Sciences, University of Zagreb

ABSTRACT
The construction of urban expressways will significantly impact the travel of surrounding residents. Traffic flow assignment is a key method to address this issue. This study, therefore, addresses the impact of urban expressway construction on nearby residents' travel by proposing an optimised traffic flow assignment method. Traditional methods rely on labour-intensive OD (origin-destination) matrix acquisition, but this research introduces an OD reverse derivation model that eliminates the need for a prior matrix. Key road sections are identified using the stepwise point placement method, with peak-hour traffic volumes surveyed. An incremental assignment method generates a distribution matrix, and the original OD matrix is derived using a maximum entropy-based model. A stochastic user equilibrium assignment model incorporating a path length-corrected logit is constructed, and a genetic algorithm solves the objective function. Using evening peak traffic data from Huai'an's road network, including an expressway construction zone, the results show that total travel time decreased by 14.11% after applying the method, from 4,050,327.517 seconds to 3,478,967.635 seconds. This demonstrates the proposed method's effectiveness in reducing congestion and improving travel efficiency for surrounding residents.

KEYWORDS
construction zone road network; maximum entropy OD inversion; traffic flow distribution; path length correction.

1. INTRODUCTION

In recent years, the construction of urban transportation infrastructure has been accelerating, with new construction, renovation and expansion projects taking up limited road space. During these construction projects, work zones are set up around the roads, occupying driving space. The complex road conditions during construction can easily trigger traffic accidents and cause traffic congestion during peak hours, creating bottlenecks in urban roads [1, 2]. According to relevant research, construction work zones not only affect road traffic flow and safety but also impact the travel of nearby residents [3-5]. Therefore, using reasonable management methods and measures, fully leveraging the efficiency of the road network, and regulating and guiding traffic flow are crucial for alleviating the conflict between traffic supply and demand, and easing local traffic pressure.

Urban expressways are the main structural framework of urban road traffic, providing a fast and efficient driving environment for motor vehicles. These expressways, free from intersecting lines, have high operational speed and capacity. With the acceleration of urbanisation in recent years, road networks in cities at all levels have been continuously improving, and many small to medium-sized cities are gradually constructing urban expressways. Expressways are typically built using elevated bridge structures, which can significantly impact

the operation of traditional urban roads during construction, leading to road blockages, traffic accidents and inconvenience for city residents. The construction on urban expressways will affect traffic on certain sections, reducing the capacity of many roads and even leading to the complete closure of some. This will cause a significant increase in traffic on parallel or alternative routes, especially during peak hours, leading to severe congestion and longer travel times across the entire road network.

With the increase in traffic demand, transportation planners can address traffic congestion through two approaches [6]. (1) Expanding infrastructure: this involves extending the road network to accommodate the growing demand. However, the application scenario of this study focuses on the impact of urban expressway construction on the urban road network, which is a temporary issue. Thus, expanding infrastructure is not adopted as a solution. (2) Using intelligent transportation systems (ITS): many studies have explored ITS-based attempts to mitigate congestion, with traffic flow assignment being a critical method to address these issues. Traffic flow assignment is the final stage of the four-step transportation planning process [7].

Performing traffic flow assignment requires obtaining the OD (origin-destination) matrix for the entire road network. Traditional OD matrix surveys are complex, requiring the division of the road network into multiple zones. Surveys typically involve questionnaires or postcard methods, where survey quality is significantly influenced by the design of the questionnaire and the surveyors. Moreover, respondents often experience a heavy burden, leading to low success rates and consuming considerable time and manpower [8, 9].

OD reverse derivation can significantly reduce the labour, financial costs and time required for large-scale OD surveys. Its principle is based on the assumption that the computational steps from the OD table to link traffic volumes can be reversed. This study attempts to use OD reverse derivation [10, 11] to obtain the OD matrix, which is then applied in traffic flow assignment methods for distribution.

Traffic flow assignment is primarily categorised into two types: deterministic traffic flow assignment models and stochastic traffic flow assignment models [12, 13]. Deterministic models assume that travellers have complete knowledge of road conditions and can make entirely accurate choices. In contrast, stochastic models consider that travellers' perception of travel time on routes is subject to error. Stochastic traffic flow assignment models better align with drivers' actual route selection behaviour in practical applications, and this study attempts to use a stochastic traffic flow assignment model.

Traditional research has relied on mathematical methods to solve OD reverse derivation models and traffic flow assignment models. With the rapid development of intelligent algorithms, typical algorithms with similar principles, such as genetic algorithms (GA) and particle swarm optimisation (PSO), have been widely used in optimising objective functions [14, 15].

The PSO algorithm converges to the optimal solution faster compared to the GA algorithm, while the GA, with its longer history, has developed mature optimisation techniques and offers broader applicability [16]. In this study, the PSO algorithm is used to solve the relatively less complex OD reverse derivation model, improving the convergence speed. In addition, the GA algorithm is employed to solve the more complex traffic flow assignment model with numerous variables, enhancing search breadth and increasing the likelihood of obtaining the optimal solution.

For the reasons mentioned above, this study takes the case of the Huai'an expressway under construction, using the stepwise point placement method to determine the survey sections of the road network. The distribution matrix is obtained based on the incremental assignment method, and using this matrix along with traffic flow detection data for the sections, the initial Origin-Destination (OD) matrix is derived through maximum entropy OD estimation. Finally, an optimised stochastic user equilibrium assignment model is employed for the distribution study.

2. LITERATURE REVIEW

To reduce the investment of manpower and resources in traditional OD surveys, research on OD estimation can be traced back to the last century. In 1979 and 1984, Nguyen [17] and Willumsen [18] conducted research on finding the most accurate OD (origin-destination) matrix using the principle of maximum entropy. Cascetta [19] proposed a generalised least squares estimator for the original OD matrix by directly combining model estimation with traffic counts through an assignment model, explicitly considering measurement errors and temporal variability in observed flows, and validated the approach with case studies. Doblas [20] addressed the estimation and updating of observed OD matrices based on available link flow information using a nonlinear programming method corresponding to the augmented Lagrangian function, and developed an efficient algorithm to estimate the OD matrix while minimising the storage requirements for solving large

problems. In 1987, Spiess [21] and colleagues proposed a maximum likelihood model, which, by assuming that OD flows follow a Poisson distribution, finds the solution that maximises the joint probability of the likelihood function constituted by the observed flows from the OD matrix. The methods mentioned above can all be used to solve the OD matrix. However, most of these methods involve constructing models and using mathematical techniques to solve them. As the complexity of different real-world cases increases, many mathematical methods become difficult to apply, making it necessary to use more broadly applicable solution methods.

In recent years, methods for OD matrix estimation have been evolving with new algorithms continually emerging, such as those using bi-level programming [22], neural networks [23, 24], heuristic algorithms [25] and others [26]. These studies have achieved promising estimation results. However, all of the aforementioned methods require a prior OD matrix. This study considers the scenario where no prior matrix is available and seeks to derive the OD matrix by using traffic volumes from key road sections as constraints.

Traffic flow assignment is mainly divided into two categories: deterministic traffic flow assignment models and stochastic traffic flow assignment models. Deterministic traffic flow assignment models assume that travellers have complete knowledge of road conditions and can make perfectly accurate choices. On the other hand, stochastic traffic flow assignment models assume that travellers' perceptions of travel time on different paths are subject to error. The deterministic traffic flow assignment model was first proposed by Wardrop [27] and includes Wardrop's first and second principles, although the first principle is difficult to quantify. Fisk and Boyce [28] provided a variational inequality formulation for the network equilibrium route choice problem and extended existing results to models with irreversible travel demand functions. They further developed the model to account for the possibility of dispersion in route choice.

Daganzo and Sheffi [29] were the first to propose stochastic traffic flow assignment models, which are an extension of traditional deterministic traffic flow assignment models. Stochastic traffic flow assignment models are mainly divided into two categories: if the error terms in travellers' perceptions of road travel costs are assumed to be independent and follow a gamma distribution, a logit model can be derived; if the error terms are not independent and the joint distribution follows a multivariate normal distribution, a probit model can be derived. Fisk [30] was the first to propose a random equilibrium assignment model based on the logit model. Wang [31] and Yan [32], using cumulative prospect theory as the criterion for route choice, proposed a uniform distribution assignment model.

Summarising current research findings, compared to deterministic traffic flow assignment models, stochastic traffic flow assignment models are more aligned with real-world conditions as they assume that travellers' perceptions of travel time on paths are subject to error. This also provides an important insight for determining the research methods of this study. However, traditional methods using the logit model to determine route choice probability only consider the impact of travel time on route choice, while in reality, many factors influence travellers' route choices, such as travel distance, travel cost and others. In this study, in addition to considering travel time, we also take into account the impact of travel distance on travellers, making the model more realistic.

In summary, the main contributions of this study are as follows.

This study proposes an OD estimation method without a prior matrix, reducing the workload of traditional OD surveys. The new model randomly determines an initial OD matrix and uses the unbalanced distribution method to obtain a distribution matrix. By using the distribution matrix and traffic volume data from road segments, the OD matrix is estimated through maximum entropy OD estimation, and the model is solved using the particle swarm optimisation (PSO) algorithm. In this new OD estimation process, the distribution matrix is used, eliminating the need for a prior OD matrix. At the same time, the PSO algorithm provides broader adaptability, higher computational accuracy and faster computation speed compared to traditional mathematical methods.

This study also proposes a stochastic traffic flow distribution method based on the path length-adjusted logit model. Building on traditional models that only consider travel time, this new model also incorporates road segment length as an important criterion for route selection. Additionally, the stochastic traffic flow distribution model accounts for the fact that travellers' perceptions of travel time on routes are subject to errors, making the new model more consistent with real-world conditions.

The Huai'an city's expressway construction road network is used as a case study for validation. Traditional studies mostly focus on normal road network distribution, while research on construction road network distribution is relatively innovative. Construction road networks have unique characteristics: they are temporary, usually tied to the construction period of road segments, and the impacts will disappear once

construction is completed; they are also transmissible, as construction on multiple road segments can reduce or eliminate capacity on these segments, leading to congestion on parallel or alternative routes and thus causing disruption across the entire road network. These characteristics make this study highly relevant. Finally, the comparison of road network parameters before and after distribution validates that this study can reduce network congestion.

3. OD MATRIX ESTIMATION MODEL WITHOUT PRIOR MATRIX

The key road sections were selected using a step-by-step approach. The peak-hour traffic volumes of the sections were surveyed, and an OD matrix was generated randomly. The OD matrix was then assigned to various road sections within the network using the incremental assignment method, resulting in an assignment matrix. This assignment matrix, along with the surveyed traffic volumes, was incorporated into the maximum entropy-based OD estimation model, which was solved using the particle swarm optimisation algorithm to obtain the assignment matrix.

3.1 Basic principles of OD matrix estimation and selection of key survey sections

Traditional OD surveys usually require a significant amount of human and material resources. To reduce the shortcomings of large preliminary survey efforts in traffic planning, researchers have begun using traffic volumes on road segments to estimate the OD matrix. Traffic flow assignment involves distributing segment traffic volumes based on the OD matrix; therefore, OD matrix estimation is essentially the reverse process of traffic flow assignment. The method of OD matrix estimation involves deriving the current travel OD matrix for traffic zones based on the observed traffic flows of the existing road network. The expression for OD matrix estimation is shown in *Equation 1* [33]

$$\sum_i \sum_j T_{ij} P_{ij}^a = V_a,\ a = 1, \cdots, M; i, j = 1, \cdots, N \tag{1}$$

where a represents the name of a road segment, i and j are the names of zones, T_{ij} represents the traffic volume from zone i to zone j, which is the demand to be estimated by the OD matrix, P_{ij}^a represents the proportion of T_{ij} assigned to road segment a, which can be obtained through traffic assignment. This matrix has rows representing the number of road segments and columns representing the number of OD points, and V_a represents the traffic volume on road segment a, which can be obtained through actual surveys. *Equation 1* describes the relationship between OD demand and road segment traffic volumes. This equation has $N(N-1)$ unknowns and M equations. When $N(N-1)>M$, the system of equations has infinitely many solutions. Since the number of OD points in a real road network, $N(N-1)$, is usually greater than the number of road segments, M, additional constraints are needed to determine the optimal solution.

3.2 Selection of survey segments based on the stepwise point placement method

The principle of OD matrix estimation is to use observed traffic volumes on road segments to infer the OD matrix. Generally, the more segment information used, the more accurate the resulting OD matrix will be. However, this approach contradicts the original intent of keeping the OD estimation process simple and convenient. To address this issue, this study proposes a method for selecting survey segments based on the stepwise point placement method. The main steps are as follows:

— Step 1: Allocate all OD pair demands to the road network using the shortest path method.
— Step 2: Identify the road segment with the highest frequency of OD pair trips as the observation segment.
— Step 3: Remove all OD pairs that pass through the identified observation segment, and reallocate the remaining OD pairs to the road network using the shortest path method.
— Step 4: Repeat Steps 2 and 3 until all OD pairs have been removed.

This method ensures that the selected key segments provide broad coverage of segment information while keeping the survey workload manageable.

3.3 Multi-OD pair assignment model based on the incremental assignment method

The incremental assignment method involves dividing the OD demand into several portions and iteratively assigning each portion of OD demand to the shortest path on the road network. After each assignment, the impedance (resistance) of each road segment is updated. The shortest path is then recalculated based on the

new impedance, and the process is repeated, with each portion of OD demand being assigned to the shortest path. This continues until all OD demand has been allocated. The assignment matrix, P_{ij}^{a} , where rows represent road segments and columns represent OD pairs, is a crucial factor for OD matrix estimation. Each time an OD pair is assigned, the elements of each column of the assignment matrix P_{ij}^{a} are calculated using *Equation 2*

$$p_j = \frac{m_i}{T_j} \tag{2}$$

where, p_j represents the set of values in the jth column of the assignment matrix (where *j*=1, 2, …, N, with N being the number of OD points), m_i represents the traffic volume allocated to each road segment for a given OD pair (where *i*=1, 2, …, *M*, with M being the number of road segments), T_j is the traffic demand for the *j*th OD pair.

The process continues until the last OD pair is assigned, at which point all the p_j values are combined to form the assignment matrix. The detailed steps are as follows:

— Step 1: Initialise the impedance of the road segments and divide the OD demand into fixed portions.
— Step 2: Calculate the road segment impedance and assign one portion of the OD demand to the shortest path.
— Step 3: Check whether all demand between the given OD pair has been assigned. If not, move on to the next portion of demand for that OD pair and return to Step 2. If the assignment for that OD pair is complete, calculate the column values of the assignment matrix using the formula provided, and proceed to Step 4.
— Step 4: Check if all OD pairs have been fully assigned. If not, move on to the next OD pair and return to Step 2. If all OD pairs have been assigned, the final assignment matrix is generated.

3.4 Maximum entropy OD inversion model based on particle swarm optimisation algorithm

An entropy-maximising OD reverse model was established to analyse the shortcomings of the Newton iteration method and the advantages of solving with the particle swarm optimisation algorithm. Considering the presence of constraints, the Lagrange multiplier method was employed for preprocessing. Finally, the steps for solving the entropy-maximising OD reverse model using the particle swarm optimisation algorithm were determined.

Establishment of the maximum entropy OD inversion model

In the maximum entropy model [34], it is assumed that vehicle travel is random. If each OD pair's travel on T_{ij} is considered a random event, the total number of events is,

$$T = \sum_i \sum_j T_{ij} \tag{3}$$

According to the principles of permutation and combination, the methods to form the matrix $[T_{ij}]$ include,

$$W(T_{ij}) = T!/\prod_{i,j} T_{ij}! \tag{4}$$

The idea of maximum entropy is to find the matrix that maximises $W(T_{ij})$, which is considered to have the highest probability of occurrence. For ease of computation, taking the logarithm on both sides of the equation yields:

$$InW(T_{ij}) = In(T!) - \sum_i \sum_j In(T_{ij}!) \tag{5}$$

According to Stirling's approximation formula $In(x!) = x \cdot In(x) - x$, we obtain:

$$max\ E \approx InW(T_{ij}) = TIn(T) - T - \sum_i \sum_j (T_{ij} In(T_{ij}) - T_{ij}) = - \sum_i \sum_j T_{ij} In(T_{ij}/T) \tag{6}$$

In this study, to maximise the matrix $W(T_{ij})$, let $max\ E \approx InW(T_{ij})$. *Equation 1* is used as the constraint for the objective function, leading to the new OD inversion model as shown in *Equation 7*. *Equations 8* and *9* represent the constraints.

$$max\ E = -\sum_i \sum_j T_{ij} In(T_{ij}/T) \tag{7}$$

$$\sum_i \sum_j T_{ij}\, P_{ij}^a = V_a,\ a = 1, \cdots, M; i, j = 1, \cdots, N \tag{8}$$

$$T_{ij} \geq 0, \forall i, j. \tag{9}$$

Directly solving the above objective function is quite difficult; it usually requires transforming the objective function into a different form.

Handling based on the Lagrange multiplier method

Using the Lagrange multiplier method to handle the above objective function, the Lagrangian function *L* is obtained as follows:

$$L = -\sum_{i=1}^{n}\sum_{j=1}^{n} T_{ij} In(T_{ij}/T) + \sum_{a=1}^{m} \lambda_a \left(V_a - \sum_{i=1}^{n}\sum_{j=1}^{n} T_{ij} P_{ij}^a \right) \tag{10}$$

In the equation, λ_a represents the Lagrange multiplier. Taking the partial derivative of the above equation with respect to T_{ij}, we obtain *Equation 11*.

$$\partial L/\partial T_{ij} = -\,In(T_{ij}/T) - \sum_{a=1}^{m} \lambda_a\, P_{ij}^a = 0 \tag{11}$$

After solving and organising, we obtain T_{ij} as below:

$$T_{ij} = T\ exp\left(-\sum_{a=1}^{m} \lambda_a\, P_{ij}^a \right) \tag{12}$$

Let $T = exp(-\lambda_0)$, and substitute this into the objective function and constraints. This results in the following two sets of equations.

$$\begin{cases} 1 = \sum_i \sum_j exp\left(-\sum_{a=1}^{m} \lambda_a\, P_{ij}^a \right) \\ \sum_{i=1}^{n}\sum_{j=1}^{n} exp\left(-\lambda_0 - \sum_{a=1}^{m} \lambda_a\, P_{ij}^a \right) P_{ij}^a = V_a \end{cases} \quad a = 1, \cdots, m \tag{13}$$

Observing that *Equation 13* contains a nonlinear system of m+1 variables and m+1 equations, solving this system yields the unknown values $\lambda_0, \lambda_1, \cdots, \lambda_m$. Substituting these values into *Equation 12* provides the OD inversion matrix.

Solving the maximum entropy OD reverse model based on particle swarm optimisation

1) Deficiencies of the Newton iteration method for solving the maximum entropy OD reverse model

Traditional methods use the Newton iteration method to solve the above nonlinear function, as detailed in reference [35]. The main drawbacks of the Newton iteration method are:

— The initial value λ_0 needs to be close to the actual value to ensure high computational accuracy.

— The method requires the inversion of matrices during iterations, which is computationally complex and requires non-singular matrices.
— When elements in the allocation matrix P_{ij}^{a} approach zero, it can lead to ill-conditioned matrices, causing the solution to fail.

2) Advantages of solving the maximum entropy OD reverse model based on particle swarm optimisation

The main advantages of the particle swarm optimisation algorithm are:

— It does not require complex mathematical calculations. By simply determining the objective function and constraints, the algorithm can search for the optimal parameter values.
— The algorithm's computational accuracy does not depend on the initial value λ_0.
— The particle swarm optimisation algorithm usually achieves higher computational accuracy than the Newton iteration method.

3) Steps for solving the maximum entropy OD reverse model based on particle swarm optimisation

— Step 1: Determining the objective function: the particle swarm optimisation algorithm cannot directly solve nonlinear equations, so preprocessing of *Equation 13* is necessary. The purpose of solving the system of equations is to determine the values of the parameters $\lambda_0, \lambda_1, \cdots, \lambda_m$ when the function on the left side of the equation equals the value of the function on the right side. This transforms the objective function into the form shown in *Equation 14*.

$$min\, y = \left(\left(\begin{array}{c} \left(\sum_{i=1}^{n} \sum_{j=1}^{n} exp\left(-\sum_{a=1}^{m} \lambda_a P_{ij}^{a} \right) - 1 \right)^2 \\ + \sum_{a=1}^{m} \left(\sum_{i=1}^{n} \sum_{j=1}^{n} exp\left(-\lambda_0 - \sum_{a=1}^{m} \lambda_a P_{ij}^{a} \right) P_{ij}^{a} - V_a \right)^2 \end{array} \right) \Big/ (m+1) \right)^{0.5} \tag{14}$$

According to *Equation 14*, the closer the objective function is to 0, the closer the values on both sides of the nonlinear *Equation 13* are, indicating that the determined parameters $\lambda_0, \lambda_1, \cdots, \lambda_m$ are closer to the actual values.

— Step 2: Obtaining the traffic volume and allocation matrix for road segments: the traffic volume for road segments is obtained through actual surveys, and the allocation matrix P_{ij}^{a} is obtained using traffic flow allocation methods.
— Step 3: Randomly initialise the particle swarm: randomly initialise the population, with the parameters to be determined as $\lambda_0, \lambda_1, \cdots, \lambda_m$, making the dimension of each particle m+1. During the initialisation of the population, *N* vectors of dimension *m*+1 are generated as the initial positions of the particles and the initial velocities of the particles.
— Step 4: Calculation of the particle fitness value: the goal of this section is to find the values of the parameters $\lambda_0, \lambda_1, \cdots, \lambda_m$ that correspond to the minimum *y* value. *Equation 10* is used as the fitness function for this purpose.
— Step 5: Update the particle's individual best vector P_i and the global best vector P_g: the update of the individual best vector P_i and the global best vector P_g is done as described in the previous section.
— Step 6: Update the particle's velocity and position. The methods for updating particle velocity and position are detailed in references [35, 37].
— Step 7: Termination criterion: repeatedly execute Steps 4 to 6, setting the number of iterations based on the convergence curve to determine and output the values of parameters $\lambda_0, \lambda_1, \cdots, \lambda_m$ that correspond to the minimum *y* value.
— Step 8: Calculation of the OD matrix: the parameters $\lambda_0, \lambda_1, \cdots, \lambda_m$ obtained are substituted into *Equation 12* along with the allocation matrix to calculate the OD matrix.

4. OPTIMISED RANDOM USER EQUILIBRIUM ALLOCATION MODEL

A stochastic user equilibrium assignment model based on path-length-corrected logit was developed. Through theoretical proof, it was demonstrated that the stochastic user equilibrium assignment model with path-length correction is equivalent to the path choice model. The model was formulated using path traffic flow as the variable, and the path-length-corrected logit stochastic user equilibrium assignment model was solved using a genetic algorithm.

4.1 Path length-corrected logit path choice model

Traditional deterministic allocation models assume that road users are fully aware of the actual road conditions. However, in practice, road users often do not have complete information about the road conditions, which can lead to discrepancies between deterministic models and real-world conditions. To make the model more consistent with actual road conditions, this study proposes a random user equilibrium model based on a path length-corrected logit model. Traditional random allocation methods use the logit model to determine the probability of each path being chosen, with the main calculation method shown in *Equation 15* [36]

$$p_k^{rs} = e^{-\theta \cdot c_k^{rs}} \Big/ \sum_{l \in K^{rs}} e^{-\theta \cdot c_l^{rs}} \tag{15}$$

where $-\theta \cdot c_k^{rs}$ represents the utility function in the logit model, and p_k^{rs} denotes the probability of path k being chosen for the OD pair rs; c_k^{rs} is the expected perceived travel cost for path k between rs (typically replaced by path travel time); K^{rs} represents the set of paths for the OD pair rs, and l denotes any path for the OD pair rs; θ is a positive dispersion coefficient parameter.

From the model, it can be observed that the smaller the path travel time c_k^{rs}, the larger the probability p_k^{rs} of choosing that path, which aligns with real-world road conditions. However, traditional random allocation models' utility functions only consider travel time's effect on path choice. To address this, this study includes path length as a factor in the utility function and proposes a new path choice probability as follows:

$$p_k^{rs} = e^{-\theta \cdot c_k^{rs} - \gamma \cdot d_k^{rs}} \Big/ \sum_{l \in K^{rs}} e^{-\theta \cdot c_l^{rs} - \gamma \cdot d_l^{rs}} \tag{16}$$

where d_k^{rs} represents the distance of path k between the OD pair rs; γ is the estimated parameter that indicates the importance of path distance in the utility function. From the model, it can be seen that the smaller the path distance d_k^{rs}, the larger the probability p_k^{rs} of choosing that path, which aligns with real-world road conditions.

4.2 Construction of the path length-corrected logit random user equilibrium allocation model

This study constructs the random user equilibrium model based on the path length-corrected logit model as shown in *Equation 17*:

$$min\, Z = \sum_a \int_0^{x_a} t_a\,(w)dw + 1/\theta \cdot \sum_{rs} \sum_k f_k^{rs}\, In(f_k^{rs}) + r/\theta \cdot \sum_{rs} \sum_k d_k^{rs} \cdot f_k^{rs} \tag{17}$$

$$\sum_k f_k^{rs} = q_{rs} \tag{18}$$

$$f_k^{rs} \geq 0 \tag{19}$$

$$x_a = \sum_r \sum_s \sum_k f_k^{rs}\, \delta_{a,k}^{rs} \tag{20}$$

where f_k^{rs} represents the flow on the *k*-th path between origin r and destination s in the OD pair. $t_\alpha()$ denotes the actual impedance of link a, the computational method is described in Step 8 of Section 4.3. q_{rs} indicates the traffic demand for the OD pair from origin *r* to destination *s*. $\delta_{\alpha,k}^{rs}$ is a 0-1 variable representing the relationship between the link and the path. If link *a* belongs to the *k*-th path of the OD pair from origin *r* to destination *s*, then $\delta_{\alpha,k}^{rs}$=1; otherwise, $\delta_{\alpha,k}^{rs}$=0. x_a denotes the traffic volume on link *a*. d_k^{rs} represents the distance of path k between OD pair *rs*. γ is the path parameter, and θ is a positive dispersion coefficient.

Here, *Equation 17* represents the objective function to be minimised; *Equation 18* describes the relationship between path flow and OD demand; *Equation 19* represents the non-negativity constraint on path flow; and *Equation 20* defines the relationship between path flow and segment flow.

Theorem 1: The random user equilibrium flow allocation and path choice model based on the path length-corrected logit model are equivalent, that is, $p_k^{rs} = e^{-\theta \cdot c_k^{rs} - \gamma \cdot d_k^{rs}} / \sum_{l \in K^{rs}} e^{-\theta \cdot c_l^{rs} - \gamma \cdot d_l^{rs}}$.

Proof: Construct the Lagrangian function for *Equation 17* as shown in *Equation 21*:

$$L = \sum_a \int_0^{x_a} t_a(w)dw + 1/\theta \cdot \sum_{rs} \sum_k f_k^{rs} In(f_k^{rs}) + r/\theta \cdot \sum_{rs} \sum_k d_k^{rs} \cdot f_k^{rs} + \sum_{rs} \lambda_{rs} \left(q_{rs} - \sum_k f_k^{rs} \right) \tag{21}$$

where λ_{rs} is the Lagrange multiplier for the constraint. *Equation 21* satisfies the Kuhn-Tucker conditions, meaning that it meets $f_k^{rs} \cdot \partial L / \partial f_k^{rs} = 0$ and $\partial L / \partial f_k^{rs} \geq 0$ conditions. From this, *Equations 22* and *23* can be derived.

$$f_k^{rs} \cdot (C_k^{rs} + 1/\theta \cdot (In(f_k^{rs}) + 1) + \gamma/\theta \cdot d_k^{rs} - \lambda_{rs}) = 0 \tag{22}$$

$$C_k^{rs} + 1/\theta \cdot (In(f_k^{rs}) + 1) + \gamma/\theta \cdot d_k^{rs} - \lambda_{rs} \geq 0 \tag{23}$$

For each valid path *k* between the OD pair *rs* where $f_k^{rs} > 0$, it follows that:

$$C_k^{rs} + 1/\theta \cdot (In(f_k^{rs}) + 1) + \gamma/\theta \cdot d_k^{rs} - \lambda_{rs} = 0 \tag{24}$$

Solving for f_k^{rs} according to *Equation 24* yields the following expression:

$$f_k^{rs} = e^{\theta \lambda_{rs} - 1} \cdot e^{-\theta c_k^{rs} - r d_k^{rs}} \tag{25}$$

Summing over all paths between the OD pairs in *Equation 24* yields:

$$\sum_l f_k^{rs} = \sum_l e^{\theta \lambda_{rs} - 1} \cdot e^{-\theta c_l^{rs} - \gamma d_l^{rs}} \tag{26}$$

Based on *Equations 25* and *26*, the path choice probability for the path length-corrected logit model is given by the following expression.

$$p_k^{rs} = f_k^{rs} / q^{rs} = e^{-\theta c_k^{rs} - r d_k^{rs}} \Big/ \sum_l e^{-\theta c_l^{rs} - \gamma d_l^{rs}} \tag{27}$$

From *Equation 17* and the proven result in *Equation 27*, it is demonstrated that the random user equilibrium flow allocation and path choice model based on the path length-corrected logit model are equivalent, thus proving the equivalence.

4.3 Solving the random user equilibrium allocation model based on genetic algorithms

— Step 1: Determination of the objective function

Substitute the road segment traffic volume calculation equation into the objective function, using path traffic volume as the variable. The modified objective function is given by *Equation 28*.

$$min\, Z = \sum_a \int_0^{\sum_r \sum_s \sum_k f_k^{rs} \delta_{a,k}^{rs}} t_a(w)dw + 1/\theta \cdot \sum_{rs} \sum_k f_k^{rs} In(f_k^{rs}) + \gamma/\theta \cdot d_k^{rs} \cdot f_k^{rs} \tag{28}$$

— Step 2: Determination of parameters related to the objective function

Identify the length of each road segment in the network, the set of all paths between OD points, and the free-flow travel time and capacity of each road segment.

— Step 3: Chromosome encoding

The variables in this study are the traffic volumes for each path. To facilitate operations such as selection, crossover and mutation, binary encoding is used. The accuracy of the encoding for each value, denoted as τ, can be determined using *Equation 29*

$$\tau = \frac{\sigma_{max} - \sigma_{min}}{2^{\varpi} - 1} \tag{29}$$

where ϖ represents the encoding length of a binary number; σmin_{max} indicates the range of the decimal values for the parameters to be determined. After converting the binary number to a decimal, multiplying by the encoding precision yields the decimal value represented in the genetic algorithm.

— Step 4: Initial population generation

Create *N* initial populations at random, where the population size generally ranges from ω to 2ω.

— Step 5: Fitness calculation

Calculate the fitness of each individual in the population. This is usually the objective function of the genetic algorithm, and the fitness function serves as the main criterion for "survival of the fittest". An individual with higher fitness has a greater probability of being passed on to the next generation, while an individual with lower fitness has a lower probability of being inherited. The goal of this study is to find the traffic volumes for each path that minimise the objective function, as shown in *Equation 28*.

– Step 6: Selection, crossover and mutation operations

1) Individuals with higher fitness are generally given more opportunities to be passed on to the next generation. This study employs the Monte Carlo method to determine each individual's survival probability, thereby establishing the connection between fitness and survival likelihood. The Monte Carlo method acts as a bridge between fitness and survival probability, with the calculation provided in *Equation 30*

$$P_j = \frac{f_j}{\sum_{i=1}^{N} f_i} j = 1,2,\cdots,N \tag{30}$$

where P_j represents the survival probability of the *j*-th individual, f_j denotes the fitness function value of the *j*-th individual, and *N* is the number of individuals in the population.

2) Crossover: crossover refers to the operation of replacing and recombining parts of two parent individuals to generate new individuals. The crossover operator plays a core role in genetic algorithms. To reduce the time complexity of the crossover process, single-point crossover is used, with a crossover probability typically ranging from 0.4 to 0.99. The specific process for crossover is as follows. For any two adjacent individuals, first determine whether crossover will occur based on probability. If crossover does not occur, the two individuals remain unchanged; if crossover does occur, select a crossover point and exchange the encoding beyond that point.
3) Mutation: mutation entails altering gene values at specific locations within individual strings in the population to preserve genetic diversity and avoid the algorithm becoming trapped in local optima. The mutation probability, *pm*, generally ranges between 0.0001 and 0.1. The mutation process typically involves selecting individuals for mutation based on probability, identifying mutation points on these individuals and flipping the gene values – changing 1 to 0 and vice versa.

— Step 7: Termination criteria

Repeatedly perform fitness calculation, selection, crossover and mutation operations until a satisfactory solution is obtained or the pre-set number of iterations *T* is reached. Output the path traffic volumes corresponding to the minimum objective function value.

— Step 8: Output of path traffic volumes

Output the traffic volumes for each path after allocation. Use *Equation 20* to calculate the traffic volumes for each road segment. Based on the segment traffic volumes and using the BPR function, determine the road segment travel times. The BPR function, developed by the U.S. Federal Highway Administration, is shown below. Compare the traffic volumes and travel times before and after allocation to verify the effectiveness of the traffic flow distribution proposed in this study. To ensure that the BPR function accurately reflects the real road conditions in Huai'an, the parameters α and β in *Equation 31* were calibrated according to the method in reference [37], resulting in the new BPR function as shown in the following *Equation 32*

$$t/t_0 = 1 + a(Q/C)^{\beta} \tag{31}$$

$$t/t_0 = 1 + 0.3915(Q/C)^{1.1515} \tag{32}$$

where t is the road segment travel time and denotes the actual impedance, $t_0$is the free-flow travel time of the segment (the road travel time with no other vehicles affecting it), Q is the traffic volume of the segment, and C is the capacity of the segment; and α and β are for undetermined parameters.

5. HUAI'AN ROAD NETWORK INCLUDING EXPRESSWAY CONSTRUCTION ZONES

The rapid road construction area in Huai'an City was analysed. The study area of the road network was determined based on the construction sections, and the traffic volume on the road network links was surveyed. The traffic capacity of each link was calculated, and the OD matrix was obtained using the maximum entropy-based OD estimation model. Finally, the OD matrix was assigned, and the road traffic parameters before and after the assignment were compared.

5.1 Selection of the road network including construction zones regarding the traffic volume

The construction of expressways can significantly impact the travel of residents in the surrounding areas. This chapter selects the road network enclosed by the construction sections of the Huai'an expressway to study the traffic conditions within this network. The construction road network is illustrated in *Figure 1*.

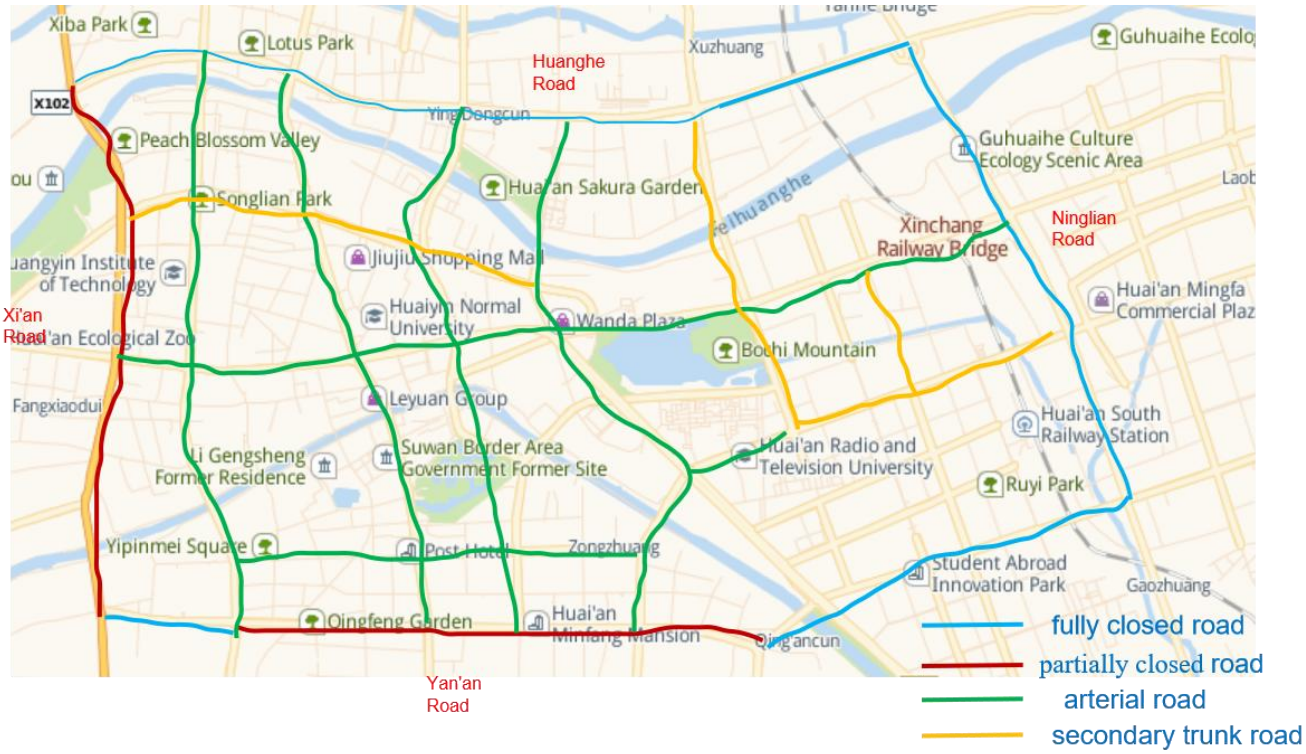

Figure 1 – Selection of construction road network and road conditions

According to *Figure 1*, the construction area includes Huanghe Road, Ninglian Road, Xi'an Road and Yan'an Road. Based on field surveys, among these construction sections, only Yan'an East Road (between Huaihai South Road and Chengde South Road) has traffic capacity. Other construction sections are either completely closed or partially closed. The partially closed roads are in poor condition and have essentially lost their traffic capacity. Fully closed sections are represented by blue lines, and partially closed sections by red lines.

This study does not consider sections that have lost their traffic capacity and primarily focuses on the distribution of traffic flow across the road network, including the construction area. The network comprises 29 major nodes and 37 road sections, considering only one-way traffic. Green lines represent primary roads, and yellow lines represent secondary roads. Basic road segment information is shown in *Table 1*, and the network topology is illustrated in *Figure 2*. The survey was conducted on 13 March 2019, from 17:00 to 18:00, covering the evening peak period. Traffic volume data for various vehicle types on all 37 road sections were collected, as shown in *Figure 3*.

Table 1 – Road segment information in the network

Road section number	Road section name	Road section location	Number of lanes (one-way)	Road length (km)	Transportation form
1	Beijing North Road	Huanghe Road - Health Road	Two lanes	1.26	separating motor and non-motor
2	Huaihai North Road	Huanghe Road - Health Road	Three lanes	1.35	separating motor and non-motor
3	Chengde North Road	Huanghe Road - Health Road	Two lanes	1.44	separating motor and non-motor
4	Xiangyu North Road	Huanghe Road - Health Road	Two lanes	1.58	separating motor and non-motor
5	Healthy West Road	Xi'an Road - Beijing Road	Two lanes	0.72	separating motor and non-motor
6	Healthy West Road	Beijing Road- Huaihai Road	Two lanes	1.05	separating motor and non-motor
7	Healthy East Road	Huaihai Road Chengde Road	Two lanes	1.09	separating motor and non-motor
8	Healthy East Road	Chengde Road-Xiangyu Road	Two lanes	1.03	separating motor and non-motor
9	Beijing North Road	Health Road - Huaihai Road	Two lanes	1.65	separating motor and non-motor
10	Huaihai North Road	Health Road - Huaihai Road	Three lanes	1.42	separating motor and non-motor
11	Chengde North Road	Health Road - Huaihai Road	Two lanes	0.826	separating motor and non-motor
12	Xiangyu North Road	Health Road - Huaihai Road	Three lanes	0.464	separating motor and non-motor
13	Nanchang North Road	Huanghe Road - Shuidukou Road	Two lanes	1.89	separating motor and non-motor
14	Huaihai West Road	Xi'an Road - Beijing Road	Two lanes	0.664	separating motor and non-motor
15	Huaihai West Road	Beijing Road-Huaihai Road	Two lanes	1.56	separating motor and non-motor
16	Huaihai East Road	Huaihai Road-Chengde Road	Three lanes	0.964	separating motor and non-motor
17	Huaihai East Road	Chengde Road-Xiangyu Road	Three lanes	0.850	separating motor and non-motor
18	Shuidukou Road	Xiangyu Road-Nanchang Road	Two lanes	1.82	separating motor and non-motor
19	Shuidukou Road	Nanchang Road -Hefei Road	Two lanes	1.15	separating motor and non-motor
20	Shuidukou Road	Hefei Road-Ninglian Road	Two lanes	1.36	separating motor and non-motor
21	Beijing North Road	Huaihai Road-Jiefang Road	Two lanes	1.87	separating motor and non-motor
22	Huaihai South Road	Huaihai Road-Jiefang Road	Three lanes	1.95	separating motor and non-motor
23	Chengde South Road	Huaihai Road-Jiefang Road	Two lanes	2.36	separating motor and non-motor
24	Xiangyu Road	Huaihai Road-Jiefang Road	Four lanes	2.5	separating motor and non-motor

Road section number	Road section name	Road section location	Number of lanes (one-way)	Road length (km)	Transportation form
25	Nanchang Road	Shuidukou Road - Shenzhen Road	Two lanes	1.3	separating motor and non-motor
26	Hefei Road	Shuidukou Road - Shenzhen Road	Three lanes	1.23	separating motor and non-motor
27	Jiefang West Road	Beijing Road -Huaihai Road	Two lanes	1.73	separating motor and non-motor
28	Jiefang East Road	Huaihai Road- Chengde Road	Two lanes	0.9	separating motor and non-motor
29	Jiefang East Road + Tianjin Road	Chengde Road -Xiangyu Road	Two lanes	1.99	separating motor and non-motor
30	Shenzhen Road	Xiangyu Road - Nanchang Road	Two lanes	0.99	separating motor and non-motor
31	Shenzhen Road	Nanchang Road- Hefei Road	Three lanes	1.15	separating motor and non-motor
32	Shenzhen Road	Hefei Road -Ninglian Road	Two lanes	1.53	separating motor and non-motor
33	Beijing South Road	Jiefang Road-Yan'an Road	Two lanes	0.568	separating motor and non-motor
34	Huaihai South Road	Jiefang Road-Yan'an Road	Three lanes	0.682	separating motor and non-motor
35	Chengde South Road	Jiefang Road-Yan'an Road	Three lanes	0.712	separating motor and non-motor
36	Tianjin Road	Jiefang Road-Yan'an Road	Two lanes	0.754	separating motor and non-motor
37	Yan'an East Road	Huaihai Road- Chengde Road	One lane	0.81	mixed traffic

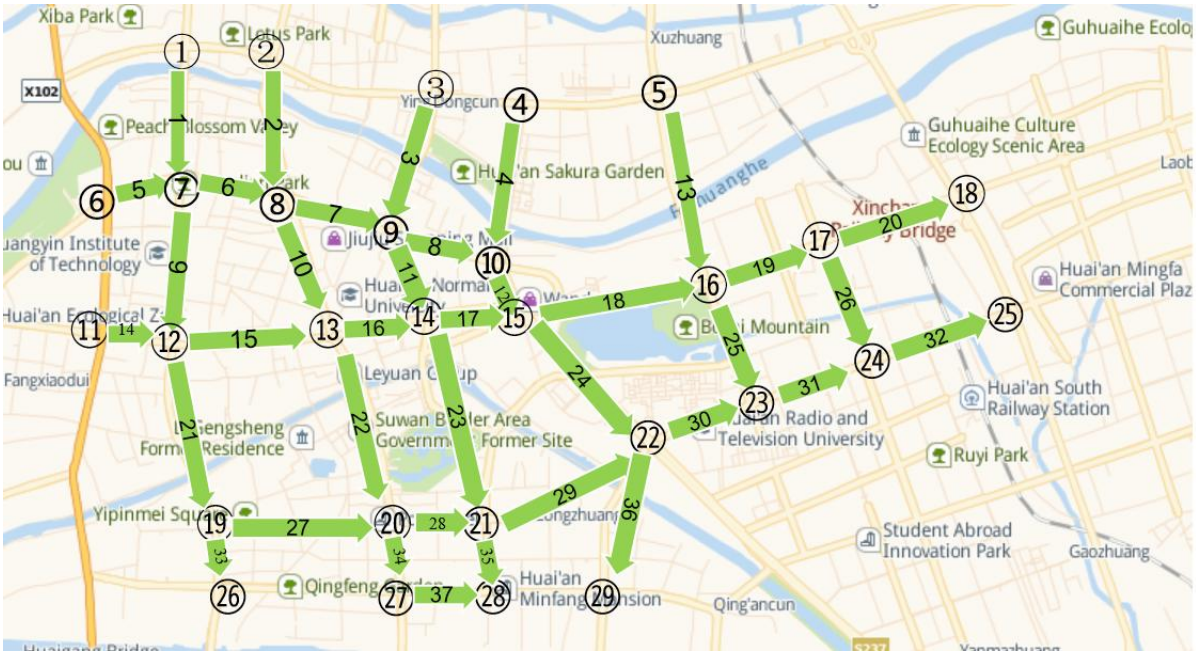

Figure 2 – Network topology diagram

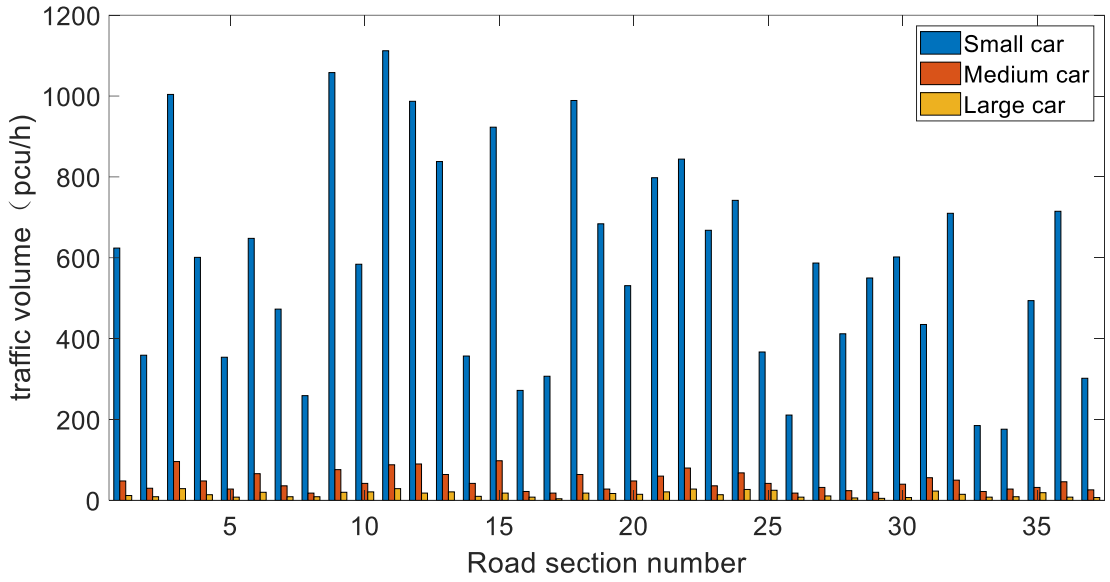

Figure 3 – Traffic volume data by vehicle type for each road section during the evening peak period

It is known that various vehicle types are present on the roads. To reduce the complexity of the assignment model and standardise the processing of traffic volume data, it is necessary to convert the above vehicle types into standard vehicle types to obtain the equivalent standard vehicle count for each road section. The conversion factors are determined based on the road occupancy level of each vehicle type. The specific conversion standards are shown in *Table 2*.

Table 2 – Traffic volume survey vehicle classification and vehicle conversion factor (TRB 2010)

Classification			Load capacity	Conversion factor	Vehicle type
Motor vehicle	Truck	Small truck	Loading ≤ 2 tons	1.0	Small
		Medium truck	2 tons < Loading ≤ 7 tons	1.5	Medium
		Large truck	7 tons < Loading ≤ 14 tons	2.0	Large
		Extra-large truck	Loading > 14 tons	3.0	N/A
		Trailers, container truck		3.0	N/A
	Bus	Minibus	Number of seats ≤ 19 seats	1.0	Small
		Large bus	Number of seats > 19 seats	1.5	Medium
		Motorcycle		0.5	N/A

The surveyed road sections are located in urban areas and do not include vehicles such as large trucks, trailers or container trucks. The table provides three vehicle categories: small vehicles, medium vehicles and large vehicles, along with their corresponding conversion factors. Using the traffic volume data for each vehicle type obtained from *Figure 3* and calculating based on the formula below, the total traffic volume data for each road section are shown in *Figure 4*.

$$Q_{\text{total}} = Q_{small} + \rho \cdot Q_{medium} + \mu \cdot Q_{large} \tag{33}$$

where Q_{total} is the total traffic volume, ρ is the conversion factor for medium-sized vehicles (1.5 has been applied), μ is the conversion factor for large vehicles, which is taken as 2 for this study, Q_{small} is the traffic volume of standard cars, Q_{medium} is the traffic volume of medium-sized vehicles, and Q_{large} is the traffic volume of large vehicles.

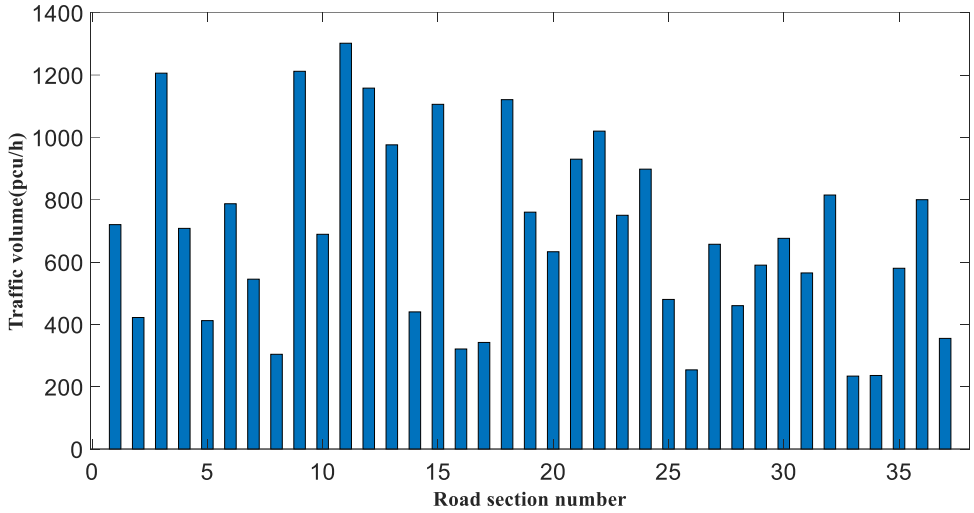

Figure 4 – Traffic volume data for road segments during the evening peak hour

According to *Figures 1, 2* and the actual road network conditions, nodes 1, 2, 3, 4 and 5 are located on Huanghe Road, which is fully closed, and there are no road segments connecting the construction points. Nodes 6 and 11 are located on Xi'an Road, which is partially closed with minimal vehicle traffic. The traffic between Node 6 and Node 11 primarily consists of local residents traveling to and from their homes and does not serve the function of a main road. The traffic volume is relatively low, so it is determined that Node 6 and Node 11 are not connected. Nodes 18 and 25 are located on Ninglian Highway, which is fully closed, with no road segments connecting the construction points. Nodes 26, 27, 28 and 29 are located on Yan'an Road; apart from the connection between nodes 27 and 28, other nodes are not connected. Conditions with partially semi-enclosed traffic volumes are as shown in *Figure 5*.

(a) *(b)*

Figure 5 – Partial semi-enclosed road condition: a) Xi'an Road conditions; b) Yan'an Road conditions (excluding the section between Huaihai South Road and Chengde South Road)

This study uses nodes 1, 2, 3, 4, 5, 6 and 11 as the starting points, and nodes 18, 25, 26, 27, 28 and 29 as the endpoints, considering only unidirectional traffic. There are 32 effective OD pairs, with a total of 152 valid paths between the OD pairs. The traffic volumes for each segment before allocation are shown in *Figure 4*.

Using the step-by-step point selection method, the 9 segments to be surveyed are identified as segments 1, 12, 19, 21, 22, 23, 32, 36 and 37. The peak hour traffic volumes for these 9 segments are shown in *Table 3*. In the OD estimation and traffic flow distribution, the segment impedance function uses *Equation 31*. The free-flow travel time for each segment is shown in *Figure 6*.

Table 3 – Segment traffic volumes survey

	Segment number								
	1	12	19	21	22	23	32	36	37
Volume (pcu/h)	720	1158	760	930	1020	750	815	800	355

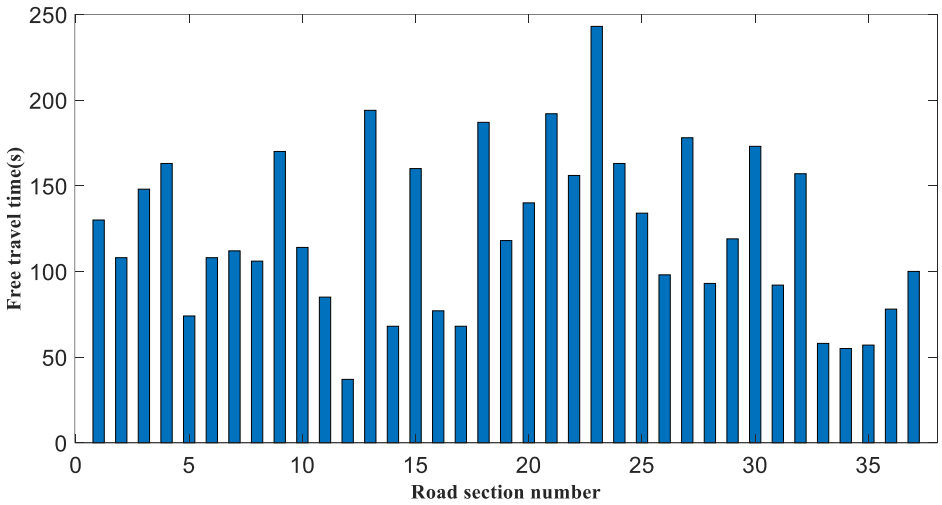

Figure 6 – Free-flow travel time for each segment

5.2 Calculation of traffic capacity for road sections within the network

To determine the traffic capacity of each road section, urban road sections are categorised into construction and non-construction sections. The traffic capacity of non-construction sections is primarily influenced by factors such as the number of lanes, lane width, proportion of non-motorised vehicles, proportion of large vehicles, intersection spacing and the number of intersections.

For construction sections, in addition to the above factors, roadwork also reduces road capacity. The influencing factors include the type of lane closures, the length of the construction area and the speed limit within the construction zone.

These influencing factors can be quantified using VISSIM simulation software. The traffic capacity of road sections can then be calculated based on a multiplicative adjustment method, as shown in the equations below [38].

Formula for calculating traffic capacity of non-construction sections

The traffic capacity of urban non-construction road sections is calculated using *Equation 34*

$$N_a = N_0 \cdot f_W \cdot f_C \cdot f_Z \cdot f_{HV} \tag{34}$$

where N_a represents the actual capacity of the road, N_0 represents the basic capacity of the road (pcu/h), determined by the impact of intersection spacing on the road segment's capacity, f_W represents the reduction factor for lane width, f_C represents the reduction factor for intersections, f_Z represents the reduction factor for non-motorised vehicles on the road segments, and f_{HV} represents the reduction factor for heavy vehicles in the work zone.

Calculation formula for traffic capacity of construction sections

The traffic capacity of urban construction sections is calculated using *Equation 35*

$$N_a = N_0 \cdot f_W \cdot f_C \cdot f_Z \cdot f_{HV} \cdot f_V \cdot f_L \tag{35}$$

where f_V represents the reduction factor for speed limits in the work zone, and f_L represents the reduction factor for the length of the construction zone.

Taking Yan'an East Road between Huaihai South Road and Chengde South Road as an example, Yan'an East Road is a construction section. According to the method described in the literature [38], the basic traffic capacity of a two-lane road with one lane closed is 1,430 pcu/h. The reduction factor for lane width is 75%, the reduction factor for non-motorised vehicles is 80%, the reduction factor for the proportion of heavy vehicles is 96%, the reduction factor for speed limits in the construction zone is 92%, and the reduction factor for the length of the construction zone is 99%. Substituting these factors into *Equation 35*, the calculated traffic capacity of Yan'an East Road is 750 pcu/h. The results for other road segments are shown in *Figure 7*.

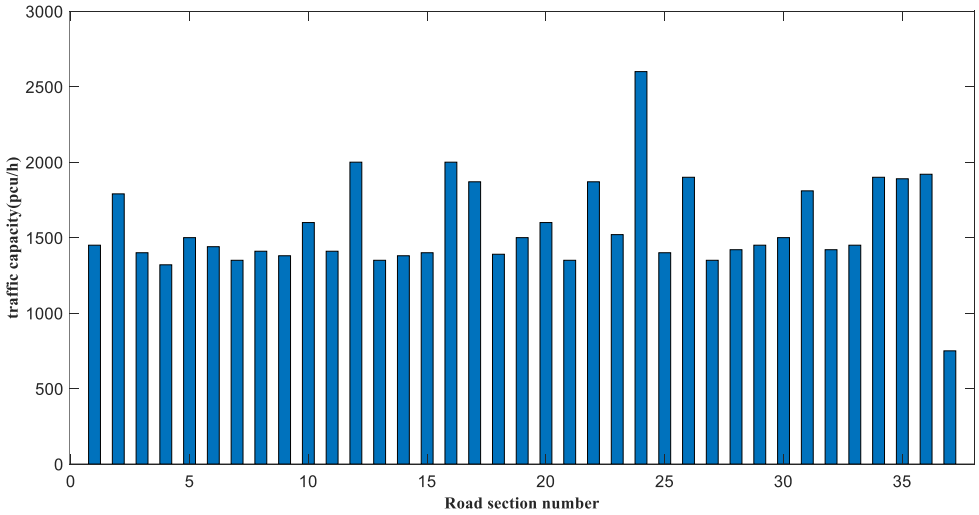

Figure 7 – Segment capacity

5.3 Calculation of the OD estimation matrix and analysis of the OD assignment results

First, set the initial demand for 32 OD pairs to 100 pcu/h. Use the incremental allocation method to sequentially allocate the traffic across the 152 valid paths between the OD points, resulting in traffic allocation outcomes T_{ij}, where i and j represent the rows and columns of the allocation results, respectively. Calculate the proportion based on the traffic flow allocation results and *Equation 2* to obtain the allocation matrix P_{ij}^{a}. Using the step-by-step point selection method, select the 9 segments with the most significant information and survey their peak hour traffic volumes. Form a new allocation matrix P_{ij}^{a} by including the rows from the incremental allocation method matrix for segments 1, 12, 19, 21, 22, 23, 32, 36 and 37. Use the survey traffic volumes and the allocation matrix P_{ij}^{a} to determine the undetermined parameter values with the maximum entropy OD estimation model, as shown in *Table 4*. The estimated OD results based on these parameters are shown in *Table 5*.

Table 4 – Parameter values

Parameter	λ_1	λ_2	λ_3	λ_4	λ_5	λ_6	λ_7	λ_8	λ_9	λ_0
Values	0.17	-0.314	2.945	1.63	2.694	0.643	1.774	2.385	-0.75	-7.24

Table 5 – Parameter values

Number	**OD point**	**OD estimation result**	**Number**	**OD point**	**OD estimation result**
1	1-18	62	17	4-25	98
2	1-25	85	18	4-29	129
3	1-26	231	19	5-18	74
4	1-27	80	20	5-25	73
5	1-28	154	21	6-18	74
6	1-29	109	22	6-25	177
7	2-18	74	23	6-26	274

Number	OD point	OD estimation result	Number	OD point	OD estimation result
8	2-25	132	24	6-27	95
9	2-27	95	25	6-28	148
10	2-28	138	26	6-29	129
11	2-29	129	27	11-18	101
12	3-18	74	28	11-25	153
13	3-25	98	29	11-26	375
14	3-28	735	30	11-27	144
15	3-29	129	31	11-28	210
16	4-18	74	32	11-29	176

Use the path-length-corrected logit random user equilibrium model to allocate traffic flow for the 32 OD pairs mentioned above. In the logit model, set the parameter θ to 2 and γ to 1. The allocated traffic for each path is shown in *Figure 8*. The traffic volume, average impedance and total vehicle travel time for each segment before and after allocation are shown in *Figure 8*.

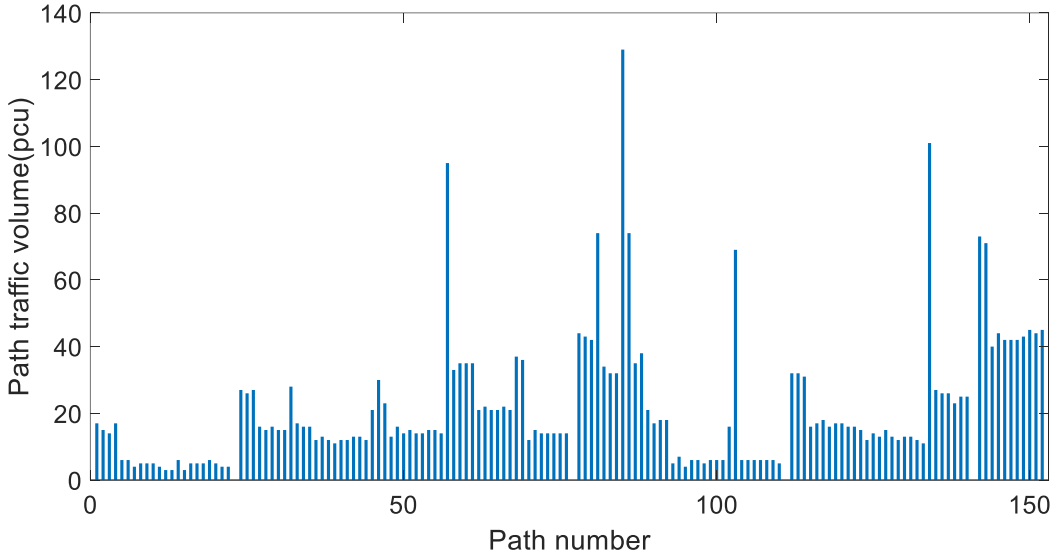

Figure 8 – Traffic volumes for each path after network allocation

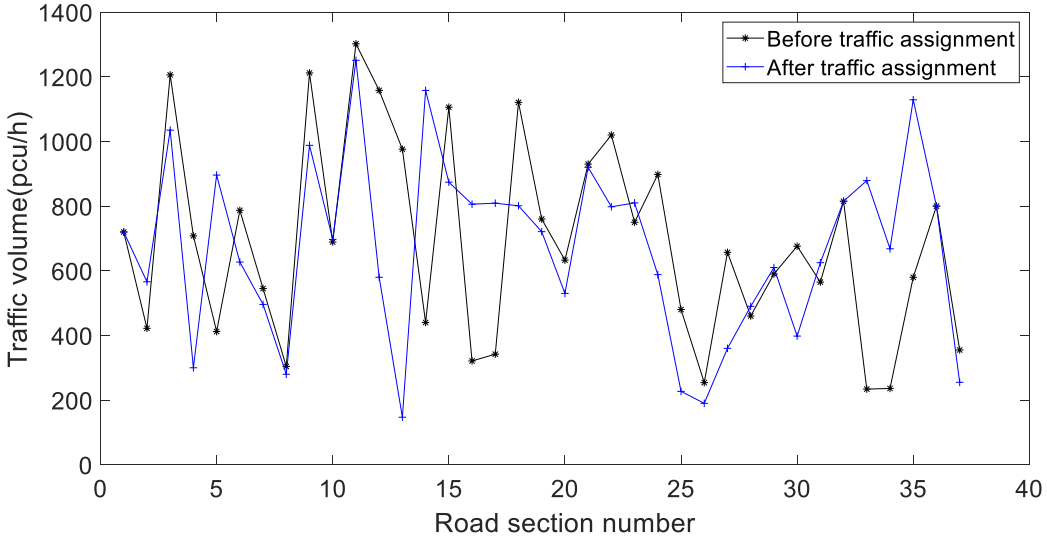

Figure 9 – Traffic volume for each segment before and after allocation

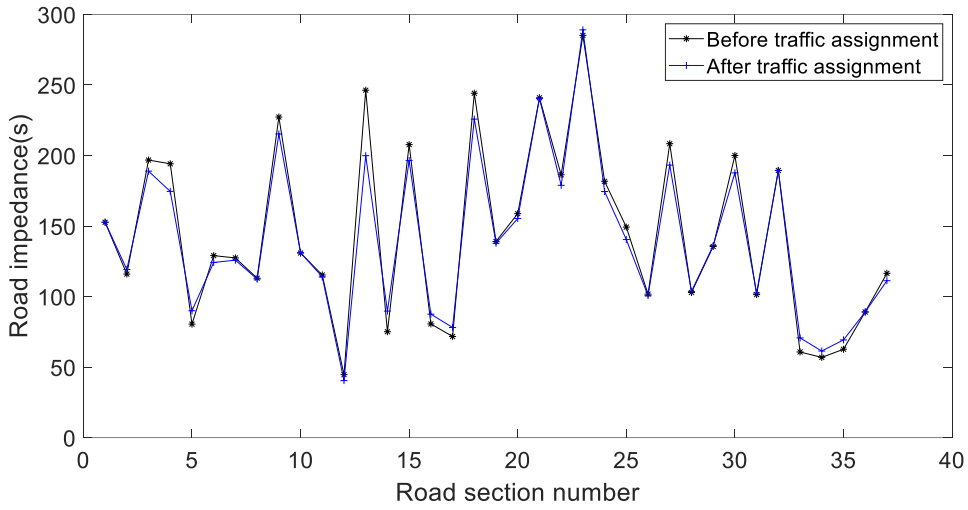

Figure 10 – Average impedance for each segment before and after allocation

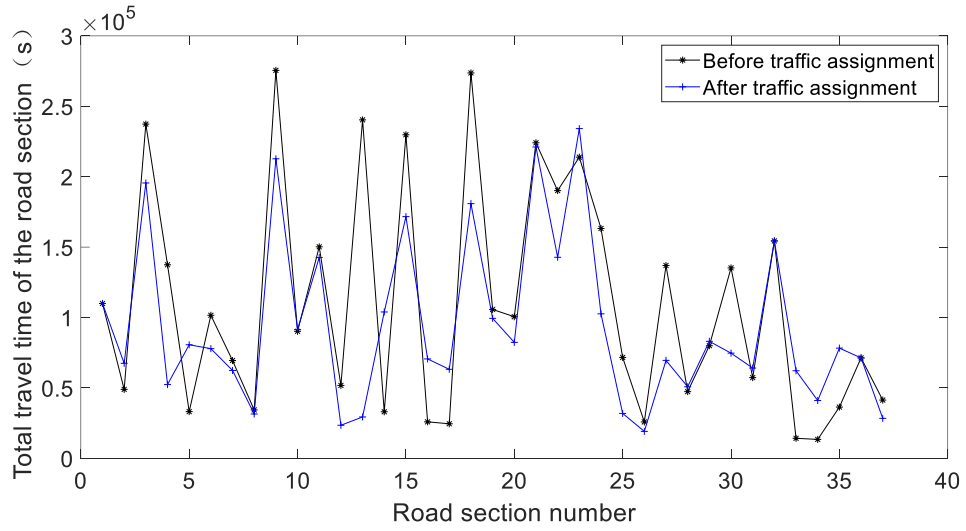

Figure 10 – Total travel time for each segment before and after allocation

According to *Figure 9*, there are significant changes in traffic volume for each segment before and after allocation, but the total traffic volume across all segments does not vary much. Specifically, traffic volumes on segments 3, 4, 6, 7, 8, 9, 11, 12, 13, 15, 18, 19, 20, 22, 24, 25, 26, 27, 30 and 37 show a notable decrease; traffic volumes on segments 1, 10, 21, 28, 29, 32 and 36 remain relatively unchanged; while traffic volumes on other segments show a significant increase. Overall, the changes in traffic volume after allocation are mainly influenced by the combined effect of free-flow impedance. Segments with smaller free-flow impedance and higher capacity receive more traffic, whereas segments with larger free-flow impedance have their traffic redirected to other segments.

According to *Figure 10*, the average impedance for each segment before and after allocation remains relatively stable. This is because the traffic volume on each segment is less than its capacity, meaning that changes in traffic volume have a minimal impact on travel time when the volume is below capacity. According to *Equation 31*, this study only considers the effect of segment traffic volume on travel time, so the changes in average impedance before and after allocation are consistent with the changes in traffic volume as shown in *Figure 9*. Specifically, for the same segment, a higher traffic volume leads to longer travel time, and a lower traffic volume leads to shorter travel time, approaching free-flow travel time.

Figure 11 shows the total travel time for each segment, calculated as the product of traffic volume and average impedance. The objective of this study is to reduce the overall network travel time. From *Figure 11*, it can be seen that for some segments, the total travel time increased after allocation, while for others, it decreased. However, the total travel time for segments 9, 13, 15 and 18 showed a notable reduction before allocation. This indicates that traffic flow allocation significantly alleviated congestion in these segments. The total

network travel time before allocation was 4,050,327.517 seconds, while after allocation it was 3,478,967.635 seconds, representing a 14.11% reduction. This suggests that the optimised traffic flow allocation method can improve traffic conditions during peak hours in construction areas.

6. CONCLUSION

In the study of traffic flow allocation for construction zone networks, many scholars have developed a substantial body of research. Building on previous studies, this study proposes an OD estimation model without a priori matrices. Based on the original OD matrix obtained through OD estimation, a random user equilibrium allocation model with path length correction logit is used for allocation research. Taking the road network in Huai'an City, which includes a construction zone on a freeway, as a case study, the results show that the overall network travel time was reduced by 14.11%, indicating that the random user equilibrium allocation model with path length correction logit can decrease vehicle travel time across the network.

However, some limitations of this study need to be acknowledged, and improvements can be made through more comprehensive work. The road travel time in the traffic flow allocation used the BPR function proposed by the American Highway Administration. Since the conditions of urban road segments in the U.S. differ significantly from those in China, although parameters were recalibrated, the study only considered the impact of segment traffic volume on travel time. Future research will focus on optimising the impedance function based on actual road conditions and incorporating more influencing factors into the impedance function calculation. Additionally, to reduce computational complexity, this study used the average impedance during peak hours as the average travel time for segments. However, traffic volumes change rapidly during peak hours, and traffic conditions vary significantly across different time periods, leading to substantial changes in travel time. Future studies will need to conduct traffic volume surveys by time periods and use appropriate mathematical methods to determine the segment impedance during peak hours, making the allocation results more aligned with actual conditions.

ACKNOWLEDGEMENTS

This work was funded by the Construction project of "Excellent Science and Technology Innovation Team in Jiangsu Province Universities, China" advanced manufacturing technology team for electronic precision molds; 2022 The General Program of Philosophy and Social Science Research in Colleges and Universities in Jiangsu Province (Grant no. 2022SJYB1969). Huai'an Basic Research Plan (Joint Special Project) Project (Grant no. HABL2023027); Jiangsu Province Key Technology Innovation Project Orientation Plan (2022) (Grant no. 1184); 2025 Huai'an Social Science Research Project (Grant no. 2025SK82).

REFERENCES

[1] Brusselaers N, Huang H, Macharis C, Mommens K. A GPS-based approach to measure the environmental impact of construction-related HGV traffic on city level. *Environmental Impact Assessment Review*. 2023;98:106955. DOI: 10.1016/j.eiar.2022.106955.

[2] Bidkar O, Arkatkar S, Joshi G, Easa SM. Effect of construction work zone on rear-end conflicts by vehicle type under heterogeneous traffic conditions. *Journal of transportation engineering, Part A: Systems*. 2023;149(4):05023001. DOI: 10.1061/JTEPBS.TEENG-7275.

[3] Ma R, Liu N. Simulation study on the influence of metro occupation construction on road capacity of mixed traffic intersection. In Second International Conference on Applied Statistics, Computational Mathematics, and Software Engineering (ASCMSE 2023) 2023; 12784: 450-459. DOI: 10.1117/12.2692077.

[4] Yu C. Study on traffic organization strategy for occupying-road construction of Qingkou interchange on Shenhai expressway. In IOP Conference Series: Earth and Environmental Science. 2021;820(1):012017. DOI: 10.1088/1755-1315/820/1/012017.

[5] Yan Z, Li L, Chen F, Xu Z. Study of expressways with heavy traffic flow during occupying-road construction. SPIE, In International Conference on Smart Transportation and City Engineering. 2021;12050:353-358. DOI: 10.1117/12.2614115.

[6] Morandi V. Bridging the user equilibrium and the system optimum in static traffic assignment: A review. *4OR*. 2024;22(1):89-119.

[7] Xu X, et al. A unified dataset for the city-scale traffic assignment model in 20 US cities. *Scientific data*. 2024;11(1):325.

[8] Hazelton ML, Najim L. Using traffic assignment models to assist Bayesian inference for origin–destination matrices. *Transportation Research Part B: Methodological*. 2024;186:103019. DOI: 10.1016/j.trb.2024.103019.

[9] Rong C, Ding J, Li Y. An interdisciplinary survey on origin-destination flows modeling: Theory and techniques. *ACM Computing Surveys*. 2023. DOI: 10.1145/3682058.

[10] Pamuła T, Żochowska R. Estimation and prediction of the OD matrix in uncongested urban road network based on traffic flows using deep learning. *Engineering Applications of Artificial Intelligence*. 2023;117:105550. DOI: 10.1016/j.engappai.2022.105550.

[11] Owais M. Deep learning for integrated origin–destination estimation and traffic sensor location problems. *IEEE Transactions on Intelligent Transportation Systems*. 2024;25(7): 6501-6513. DOI: 10.1109/TITS.2023.3344533.

[12] Cantarella GE, Fiori C. Multi-vehicle assignment with elastic vehicle choice behaviour: Fixed-point, deterministic process and stochastic process models. *Transportation Research Part C: Emerging Technologies*. 2022;134:103429. DOI: 10.1016/j.trc.2021.103429.

[13] Verstraete J, Tampère C. Recursive logit route choice modelling for traffic assignment. In Proceedings of 9th Symposium of the European Association for Research in Transportation. European Association for Research in Transportation. 2021.

[14] Kumar S, Gupta A, Bindal RK. Load-frequency and voltage control for power quality enhancement in a SPV/Wind utility-tied system using GA & PSO optimization. *Results in Control and Optimization*. 2024.100442. DOI: 10.1016/j.rico.2024.100442.

[15] Huang W, et al. Railway dangerous goods transportation system risk identification: Comparisons among SVM, PSO-SVM, GA-SVM and GS-SVM. *Applied Soft Computing*. 2021;109:107541. DOI: 10.1016/j.asoc.2021.107541.

[16] Bemani A, et al. Modeling of cetane number of biodiesel from fatty acid methyl ester (FAME) information using GA-, PSO-, and HGAPSO-LSSVM models. *Renewable Energy*. 2020;150:924-34. DOI: 10.1016/j.renene.2019.12.086.

[17] Nguyen S. Modele de distribution spatiale tenant compte des itineraries. *INFOR*. 1983;21(4):270-292.

[18] Willumsen LG. Estimating time-dependent trip matrices from traffic counts. In Papers presented during the Ninth International Symposium on Transportation and Traffic Theory held in Delft the Netherlands. 1984;11-13.

[19] Cascetta E. Estimation of trip matrices from traffic counts and survey data: a generalized least squares estimator. *Transportation Research Part B: Methodological*. 1984;18(4-5):289-99. DOI: 10.1016/0191-2615(84)90012-2.

[20] Doblas J, Benitez FG. An approach to estimating and updating origin–destination matrices based upon traffic counts preserving the prior structure of a survey matrix. *Transportation Research Part B: Methodological*. 2005;39(7):565-91. DOI: 10.1016/j.trb.2004.06.006.

[21] Spiess H. A maximum likelihood model for estimating origin-destination matrices. *Transportation Research Part B: Methodological*. 1987;21(5):395-412. DOI: 10.1016/0191-2615(87)90037-3.

[22] Behara KN, Bhaskar A, Chung E. A novel methodology to assimilate sub-path flows in bi-level OD matrix estimation process. *IEEE Transactions on Intelligent Transportation Systems*. 2020;22(11):6931-41. DOI: 10.1109/TITS.2020.2998475.

[23] Li C, Zheng L, Jia N. Network-wide ride-sourcing passenger demand origin-destination matrix prediction with a generative adversarial network. *Transportmetrica A: Transport Science*. 2024;20(1):2109774. DOI: 10.1080/23249935.2022.2109774.

[24] Zhang R, et al. Cognition-driven structural prior for instance-dependent label transition matrix estimation. *IEEE Transactions on Neural Networks and Learning Systems*. 2024;1-14. DOI: 10.1109/TNNLS.2023.3347633.

[25] Hussain E, Bhaskar A, Chung E. Transit OD matrix estimation using smartcard data: Recent developments and future research challenges. *Transportation Research Part C: Emerging Technologies*. 2021;125:103044. DOI: 10.1016/j.trc.2021.103044.

[26] Krishnakumari P, Van Lint H, Djukic T, Cats O. A data driven method for OD matrix estimation. *Transportation Research Part C: Emerging Technologies*. 2020;113:38-56. DOI: 10.1016/j.trc.2019.05.014.

[27] Wardrop, JG. Road paper: Some theoretical aspects of road traffic research. Proceedings of the institution of civil engineers. 1952;1(3):325-362. DOI: 10.1680/ipeds.1952.11259.

[28] Fisk CS, Boyce DE. Alternative variational inequality formulations of the network equilibrium-travel choice problem. *Transportation Science*.1983;17(4):454-463. DOI: 10.1287/trsc.17.4.454.

[29] Daganzo CF, Sheffi Y. On stochastic models of traffic assignment. *Transportation Science*. 1977;11(3):253-274. DOI: 10.1287/trsc.11.3.253.

[30] Fisk C. Some developments in equilibrium traffic assignment. *Transportation Research Part B: Methodological.* 1980;14(3):243-255. DOI: 10.1016/0191-2615(80)90004-1.

[31] Wang W, Sun HJ. Cumulative prospect theory-based user equilibrium model with stochastic perception errors. *Journal of Central South University*. 2016;23(9):2465-2474.

[32] Yan DM, GuoJ H. A stochastic user equilibrium model solving overlapping path and perfectly rational issues. *Journal of Central South University*. 2021;28(5):1584-1600.

[33] Krishnakumari P, Van Lint H, Djukic T, Cats O. A data driven method for OD matrix estimation. *Transportation Research Part C: Emerging Technologies*. 2020;113: 38-56. DOI: 10.1016/j.trc.2019.05.014.

[34] Phillips SJ, Anderson RP, Schapire RE. Maximum entropy modeling of species geographic distributions. *Ecological modelling*. 2006;190(3-4):231-259. DOI: 10.1016/j.ecolmodel.2005.03.026.

[35] Traub JF, Woźniakowski H. Convergence and complexity of Newton iteration for operator equations. *Journal of the ACM (JACM)*. 1979;26(2):250-258.

[36] Wang J, et al. Combined multinomial logit modal split and paired combinatorial logit traffic assignment model. *Transportmetrica A: Transport Science*. 2018;14(9):737-760. DOI: 10.1080/23249935.2018.1431701.

[37] Zhang S, An HK. A novel road traffic flow prediction model using hybrid Particle Swarm Optimization (PSO) and Radial Basis Function Neural Network (RBFNN). *Journal of Autonomous Intelligence*. 2023;6(2):883. DOI: 10.32629/jai.v6i2.883.

[38] Fellendorf M, Vortisch P. Validation of the microscopic traffic flow model VISSIM in different real-world situations. In transportation research board 80th annual meeting 2001 Jan (Vol. 11).